Polyhedron 62 (2013) 104–109

Contents lists available at SciVerse ScienceDirect

Polyhedron

journal homepage: www.elsevier.com/locate/poly

Silver(I) complexes with symmetrical Schiff bases: Synthesis, structural characterization, DFT studies and antimycobacterial assays

Isabela L. Paiva [a], Gustavo S.G. de Carvalho [a], Adilson D. da Silva [a], Pedro P. Corbi [b], Fernando R.G. Bergamini [b], André L.B. Formiga [b], Renata Diniz [a], Weberton R. do Carmo [a], Clarice Q.F. Leite [c], Fernando R. Pavan [c], Alexandre Cuin [a,*]

[a] Departamento de Química, Instituto de Ciências Exatas, UFJF, 36036-900 Juiz de Fora, MG, Brazil
[b] Instituto de Química, Universidade de Campinas, UNICAMP, 13083-970 Campinas, SP, Brazil
[c] Departamento Ciências Biológicas, Faculdade de Ciências Farmacêuticas, UNESP, 14800-900 Araraquara, SP, Brazil

ARTICLE INFO

Article history:
Received 11 April 2013
Accepted 21 June 2013
Available online 29 June 2013

Keywords:
Schiff bases
Anisaldehyde
Silver
Tuberculosis
Mycobacterium

ABSTRACT

Synthesis, structural and spectroscopic characterizations, molecular modeling and antimycobacterial assays of new silver(I) complexes with two Schiff bases – MBDA and MBDB – are reported. The complexes $[Ag(MBDA)_2]NO_3$, or AgMBDA, and $[Ag(MBDB)NO_3]$ or AgMBDB, were obtained by the reaction of the respective ligands with silver(I) nitrate in methanol. The Schiff bases were previously obtained by mixing ethylenediamine or 1,3-diaminopropane with *p*-anisaldehyde. The characterizations of the complexes were based on elemental (C, H and N) and thermal (TG-DTA) analyses and ^{13}C and ^{1}H NMR and FT-IR spectroscopic measurements, as well as X-ray structure determination for AgMBDA. Spectroscopic data predicted by DFT calculations are in agreement with the experimental data for the AgMBDA complex. The AgMBDA complex has a monomeric structure with a molar proportion 1:2 Ag/ligand, while AgMBDB presents a 1:1 proportion. The complexes AgMBDA and AgMBDB showed to be more effective against *Mycobacterium tuberculosis* than antibacterial agent silver sulfadiazine – SSD.

1. Introduction

Silver compounds have been used as antibacterial agents for a long time as therapeutic compounds [1]. Several silver(I) compounds have been prescribed due their topical antibacterial effects. Silver sulfadiazine (SSD), for example, is still widely used in the treatment of bacterial infections in burns and skin wounds, and diluted solutions of $AgNO_3$ are employed to prevent bacterial infections and conjunctivitis in newborns [2–4].

On the other hand, the use of metals and their salts as antimicrobial agents declined sharply in the middle of the last century upon the introduction of organic antibiotics such as penicillin. Since microorganisms still represent a risk to the public health, and also due to the resurgence of multirresistant bacterial strains, the development and optimization of new drugs are always of great interest. Tuberculosis (TB) still remains as a public health issue in the beginning of the 21st century, causing nearly 3 million deaths worldwide annually. In the developing countries TB is a leading cause of morbidity and mortality. Co-infections with human immunodeficiency virus (HIV) have been responsible for changes in the TB epidemiologic situation leading to the appearance of multi-drug resistant strains [5]. With the ever increasing problem of microbe resistance to current antimicrobial agents, there is an urgent demand for new classes of compounds that will efficiently inhibit the growth of pathogenic microorganisms.

Due to this critical situation, an intense effort is being addressed to the development of new drugs against microorganisms, particularly against *Mycobacterium tuberculosis*. Currently, there is a strong interest in silver(I) complexes with biological therapeutic

Abbreviations: NMR, Nuclear magnetic resonance; t, triplet; d, duplet; TG/DTA, Thermogravimetric/differencial thermal analyses; UV–Vis, Ultraviolet–visible; MBDA, *N,N′*-bis[(4-methoxyphenyl)methlylidene]ethane-1,2-diamine; MBDB, *N,N′*-bis[(4-methoxyphenyl)methlylidene]propane-1,3-diamine; AgMBDA, silver complex with MBDA; AgMBDB, silver complex with MBDB; SSD, Silver sulfadiazine; MIC, Minimal inhibitory concentration; CFU, colony forming unit; ATCC, American type collection cell; 7H9, broth used to growth mycobacterial species; THF, Tetrahydrofuran; DMSO, dimethylsulfoxide; $CDCl_3$, Chloroform-*d*; DFT, Density functional theory; LANL2DZ, Los Alamos National Laboratory, 2nd version on double zeta function; B3LYP, Becke 3-Lee Yang Parr functional; TD, Time dependent method; CCDC, Cambridge Crystallographic Data Centre.

* Corresponding author. Address: LQBin – Laboratório de Química BioInorgânica, Departamento de Química, Instituto de Ciências Exatas, Universidade Federal de Juiz de Fora, 36036-900 Juiz de Fora, MG, Brazil. Tel.: +55 32 3229 3310.

E-mail addresses: alexandre.cuin@ufjf.edu.br, alexandre_cuin@yahoo.com (A. Cuin).

0277-5387/$ - see front matter © 2013 Elsevier Ltd. All rights reserved.
http://dx.doi.org/10.1016/j.poly.2013.06.031

activities. Recently, silver(I) complexes with alfa-hydroxy-acids [6], aminoacids [7], benzotiazoles [8] and mercaptopurine [9], synthesized in our laboratories, have been shown to be more effective than SSD against *M. tuberculosis*. The mechanisms of antibacterial action of the Ag(I) complexes have been poorly described. However, there are three possibilities: (i) interference with electron transport; (ii) inhibition of bacterial deoxyribonucleic acid (DNA) replication caused by the Ag(I) ion, and (iii) modification of the bacterial cell membrane [6].

Schiff bases are typically obtained by condensation of amine compounds and active carboxyl groups (aldehyde and ketone) leading to –CH=N– groups [10]. Schiff base compounds have received special attention due to their simple methods of preparation and to their versatility of applications, especially in biological field [11].

Here, we describe the synthesis, structural characterization, DFT studies and biological assays of two Schiff bases named MBDA and MBDB (see Fig. 1) and their silver(I) complexes, named AgMBDA and AgMBDB, respectively. The crystal structure of AgMDBA is also reported.

2. Experimental

2.1. Materials and measurements

The starting compounds *p*-anisaldehyde (98%), ethylenediamine (>99.5%) and 1,3-diaminopropane (>99%) were purchased from Sigma–Aldrich Laboratory Co., and silver nitrate (>99%) was purchased from Acros Organics. All chemical reagents were used without further purification. Elemental analyses of C, H and N were performed on a CHNS-O EA 1110 Analyzer, CE Instruments. Thermal analyses were performed on a DTG-60 Simultaneous DTA-TG apparatus, Shimadzu, using the following conditions: synthetic air, flow rate of 50 $cm^3\ min^{-1}$ and heating rate of 10 °C min^{-1}, from 25 to 700 °C for both complexes. The IR spectra were recorded on a Spectrum 2000 FT-IR Perkin Elmer spectrophotometer in the range 4000–300 cm^{-1}. The samples were prepared as KBr pellets. The ^{13}C and ^{1}H NMR data for MBDA and AgMBDA were recorded on a Bruker 500 MHz and for MBDB and AgMBDB samples were recorded on a Bruker 250 MHz. Tetramethylsilane was used as the internal standard. All NMR samples were prepared in deuterated dimethylsulfoxide solutions – $(CD_3)_2SO$.

2.2. Synthesis of Schiff bases

To a 100 mL round bottom flask was added 55.3 mmol of ethylenediamine (3.20 mL) or 1,3-diaminopropane (4.10 mL) in 50 mL of absolute ethanol. Then, with continuous stirring, 15.1 mL (110.8 mol) of *p*-anisaldehyde was slowly added. The reaction was carried out under constant stirring at room temperature during 4 h. The precipitates were then collected by filtration, washed with distilled water and ether, and stored in a desiccator under silica. When ethylenediamine was used, a white crystalline solid was obtained (15.6 g, 52.7 mmol, 95.4% yield, MBDA). A pale yellow solid was obtained using 1,3-diaminopropane as reagent (16.5 g, 53.2 mmol, 96.2% yield, MBDB).

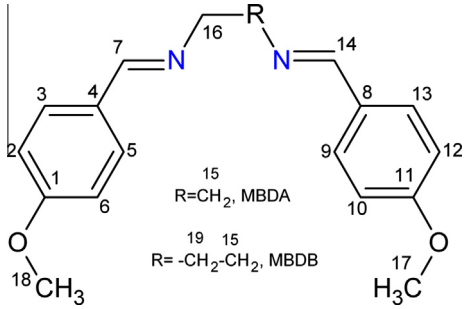

Fig. 1. Schematic structures for MBDA and MBDB.

Elemental *Anal.* Calc. for MBDA ($C_{18}H_{20}N_2O_2$): C, 72.9; H, 6.80; N, 9.45. Found: C, 73.2; H, 6.93; N, 9.90%. Elemental *Anal.* Calc. for MBDB ($C_{19}H_{22}N_2O_2$): C, 73.5; H, 7.14; N, 9.03. Found: C, 73.2; H, 6.90; N, 9.15%.

2.3. Synthesis of the Ag(I) complexes with MBDA and MBDB

2.3.1. AgMBDA complex

An ethanolic solution containing 0.592 g (2.0 mmol, 30 mL) of MBDA was first prepared. Then, a silver nitrate solution (0.170 g, 1.0 mmol), prepared in a minimum of water (~1 mL) and diluted with 10.0 mL of ethanol was added under vigorous stirring to the MBDA solution. Immediately, a yellow solid was formed. The solution was filtered and the solid was washed three times with 5 mL of cold ethanol. The solid was collected and dried in a desiccator over P_4O_{10}. The filtrate was left to stand overnight and light-yellow crystals suitable for X-rays studies were obtained. Yield ~80% (crystals plus powder). Elemental *Anal.* Calc. for $[Ag(C_{18}H_{20}N_2O_2)_2]NO_3$: C, 56.7; H, 5.29; N, 9.18; O, 14.7; Ag, 14.1. Found: C, 56.7; H, 5.38; N, 9.95; Ag, 14.3% (from the TG curve).

2.3.2. AgMBDB complex

The synthesis of AgMBDB complex was performed by the reaction of 0.310 g (1.0 mmol) of MBDB in 20 mL of THF, with a silver nitrate solution previously prepared by adding 0.0849 g of $AgNO_3$ to a mixture of water (less than 1.0 mL) and THF (10.0 mL). The silver nitrate solution was added to MBDB slowly and under stirring. A white crystalline powder was obtained. The final solution was left to stand for several days and elongated crystals were obtained. However, the crystals were not suitable for single X-ray crystallographic studies. X-ray analysis using the powder diffraction methodology are in progress. Yield ~80%. Elemental *Anal.* Calc. for $[Ag(C_{19}H_{22}N_2O_2)NO_3]\cdot\frac{1}{2}H_2O$: C, 46.6; H, 4.74; N, 8.59; O, 18.0; Ag, 22.0. Found C, 46.5; H, 4.17; N, 8.69; Ag, 21.7% (from the TG curve).

2.4. Structural characterization of the AgMBDA complex

Single-crystal data were collected using an Oxford GEMINI A-Ultra CCD diffractometer with Mo Kα (λ = 0.71073 Å) radiation at room temperature. The data collection, cell refinement and data reduction were performed using the CRYSALISPRO software [12]. The structure was solved by direct methods using SHELXS and refined using SHELXL [13]. An empirical isotropic extinction parameter x was refined according to the method described by Larson [14]. The C-bound H-atoms were included in calculated positions and treated as riding atoms using SHELXL default parameters. The non-H atoms were refined anisotropically, using weighted full-matrix least-squares on F^2. A semi-empirical absorption correction (multi-scan) was applied using CRYSALISPRO [12]. The structures were drawn using ORTEP-3 for WINDOWS [15] and MERCURY [16].

2.5. Antibacterial assays

The anti *M. tuberculosis* (anti-MTB) activities of the compounds were determined by the *Resazurin Microtiter Assay* (REMA) [17]. Stock solutions of the test compounds were prepared in dimethyl sulfoxide (DMSO) and diluted in Middlebrook 7H9 broth (Difco), supplemented with oleic acid, albumin, dextrose and catalase (OADC enrichment – BBL/Becton Dickinson, Sparks, MD, USA), to obtain final drug concentration ranges from 0.15 to 250 μg/mL. The serial dilutions were realized in a Precision XS Microplate Sam-

ple Processor (Biotek™). Isoniazid was dissolved in distilled water, as recommended by the manufacturer (Difco laboratories, Detroit, MI, USA), and used as a standard drug. MTB $H_{37}Rv$ ATCC 27294 was grown for 7–10 days in Middlebrook 7H9 broth supplemented with OADC, plus 0.05% Tween 80 to avoid clumps. Cultures were centrifuged for 15 min at 3150*g*, washed twice, and resuspended in phosphate-buffered saline. Aliquots were frozen at −80 °C. After 2 days, an aliquot was thawed to determine viability and the colony-forming unit (CFU) after freezing. MTB $H_{37}Rv$ (ATCC 27294) was thawed and added to the test compounds, yielding a final testing volume of 200 μL with 2×10^4 CFU/mL. Microplates with serial dilutions of each compound were incubated for 7 days at 37 °C, after resazurin was added to test viability. Wells that turned from blue to pink with the development of fluorescence indicated growth of bacterial cells, while maintenance of the blue color indicated bacterial inhibition. The fluorescence was read (530 nm excitation filter and 590 nm emission filter) in a SPECTRAfluor Plus (Tecan®) microfluorimeter. The MIC value is defined as the lowest concentration resulting in 90% inhibition of growth of MTB [18]. As a standard test, the MIC value for isoniazid was determined on each microplate. The acceptable MIC value for isoniazid is in the range 0.015–0.06 μg/mL. Each test was set up in triplicate and no differences were found in MIC values for each compound. All results were the same.

2.6. Molecular modeling

Geometry optimizations were carried out using the GAMESS software [19] convergence criterion of 10^{-4} a.u. in a conjugate gradient algorithm. The LANL2DZ [20] effective core potential was used for silver and the atomic 6-31G (d) basis set [21] for all other atoms. Density functional theory (DFT) calculations were performed for AgMBDA using the B3LYP [22] gradient-corrected hybrid functional to solve the Kohn–Sham equations with a 10^{-5} convergence criterion for the density charge. The molecular modeling data are presented as Supplementary material.

3. Results and discussion

3.1. IR spectroscopy

The IR spectra are shown in Fig. 2. In the MDBA and AgMBDA spectra the principal significant bands are due to coupling between C═N and C═C groups on 1640–1646 cm^{-1} and 1632 and 1609 cm^{-1} for the ligand and the complex, respectively. The shift of the absorption vibrational when the ligand and the complex spectra are compared is an evidence that the MBDA coordinates to silver(I) through the nitrogen atoms. It is also possible to observe in the MBDB and AgMBDB spectra the characteristic bands due the symmetrical and asymmetrical vibrational modes of coupling between C═N and C═C groups which occur at 1639 and 1606 cm^{-1} in the MBDB spectrum and at 1641 and 1604 cm^{-1} in the AgMBDB spectrum. The presence of the nitrate ion in both complexes were confirmed by the presence of a strong band at 1385 cm^{-1}, which is attributed to the stretching mode of NO_3 and two bands of medium intensities at 853 cm^{-1} (AgMBDA) and 835 cm^{-1} (for AgMBD), which are assigned to out-of-plane deformation of the same ion.

3.2. ^1H and ^{13}C NMR analyses

The ^1H and ^{13}C NMR spectra were obtained in order to confirm the coordination of the ligands to the metal ion by the nitrogen atoms. The spectra of AgMBDA and AgMBDB were analyzed in comparison to the NMR spectra of the free ligands. The ^{13}C and ^1H data are presented in Tables 1 and 2. Carbon and hydrogen atoms were numbered as shown in Fig. 1. Small changes in the ^{13}C NMR spectra were observed only for the carbon atoms of the azomethine groups (–C═N–), which were shifted downfield, from 162 ppm for MBDA and MBDB, to 165.7 and 163.3 ppm for AgMBDA and AgMBDB complexes, respectively. These slight changes are indicatives that the ligands are coordinated to Ag(I) ions through the nitrogen atoms.

3.3. Thermogravimetric (TG) and differential (DTA) thermal analyses

Thermal decomposition of AgMBDA was studied by TG and DTA analyses in 25–700 °C range. The endothermic peak corresponding to the melting point of complex is located at 182.7 °C. The AgMBDA complex starts to decompose at 225 °C as well as two consecutive mass losses were observed with exothermic peaks at 242 and 492 °C. The final product of thermal analysis was considered as metallic silver. The total mass loss was 85.7%, while the expected value was 85.9%.

For the AgMBDB complex, a slight mass loss is observed below 190 °C (1.82%), being attributed to the loss of hydration water (calculated 1.8%). Other two consecutive mass losses are observed (exothermic peaks at 240 and 410 °C). The endothermic peak ob-

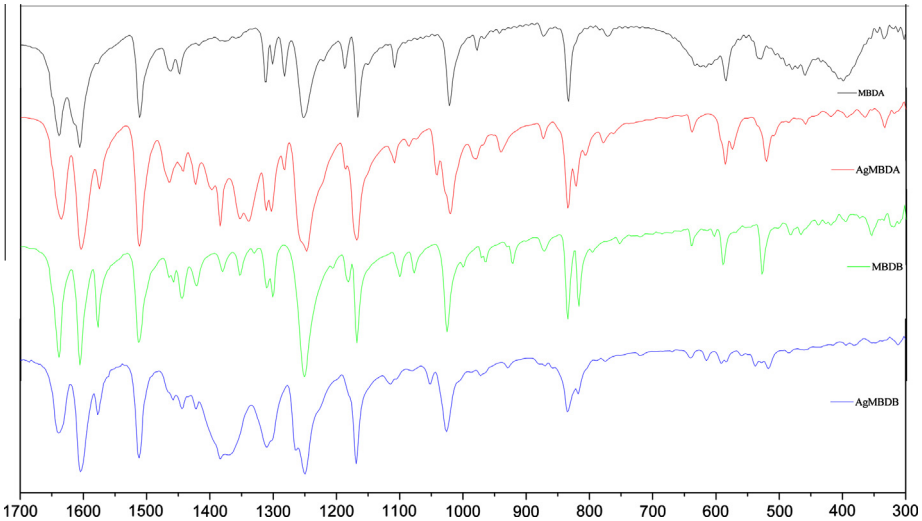

Fig. 2. Experimental FT-IR spectra for MBDA and MBDB, and their respective complexes AgMBDA and AgMBDB.

Table 1
^{1}H NMR assignments, δ and multiplicity for ligands and their Ag(I) complexes.

Assignment	MBDA (δ, ppm)	AgMBDA (δ, ppm)	Δ (δ, ppm)
7	8.23s	8.63s	−0.41
3 and 6	7.64d	7.88d	−0.24
5 and 2	6.95d	6.97d	−0.02
18	3.80s	3.78s	0.02
16	3.77s	3.94s	−0.17
	MBDB (δ, ppm)	AgMBDB (δ, ppm)	Δ (δ, ppm)
7	8.22s	8.35s	−0.13
3 and 6	7.64d	7.73d	−0.09
2 and 5	6.95d	6.93d	0.02
18	3.75s	3.76s	−0.01
16	2.48t	2.48t	0
19	1.88m	2.00m	−0.12

s = Singlet; d = doublet, t = triplet and m = multiplet. Δ Represents the difference between the chemical shifts of the complex and the free ligand.

Table 2
^{13}C NMR assignments, δ for ligands and their Ag(I) complexes.

Assignment	MBDA (δ, ppm)	AgMBDA (δ, ppm)	Δ (δ, ppm)
7	161.8	165.7	−3.9
1	161.7	163.0	−1.3
3 and 6	130.0	130.5	−0.5
4	129.7	127.4	2.3
2 and 5	114.7	114.9	−0.2
18	61.7	62.3	−0.6
16	55.9	56.2	−0.3
	MBDB (δ, ppm)	AgMBDB (δ, ppm)	Δ (δ, ppm)
7	161.6	163.3	−2.3
1	160.8	162.1	−1.3
3 and 6	129.9	132.3 and 130.0	−2.4 and −0.1
4	129.3	128.2	1.1
2 and 5	114.5	114.6	−0.1
16	58.6	59.7	−1.1
18	55.7	55.8	−0.1
19	32.4	32.6	−0.2

served at 155.3 °C on the DTA curve is due to the melting of AgMBDB. After 450 °C no mass losses were observed and the residue fits to metallic silver. The experimental mass loss was 78.3% and the expected one considering the molecular formula [Ag($C_{19}H_{22}N_2O_2$)NO_3]·½H_2O was 77.6%.

3.4. Crystallographic studies for AgMBDA

The crystallographic parameters for AgMBDA are summarized in Table 3, while selected bond distances and angles are given in Table 4. The crystal structure of AgMBDA is shown in Fig. 3. Crystals of AgMBDA contain two crystallographically independent half molecules, see the Fig. 4. One of which shows the twofold axis passing through the metal ion and the center of the two aliphatic CH_2–CH_2 vectors, the other one possessing a complete MBDA ligand bound to a silver atom lying on the twofold axis. A single nitrate ion completes the asymmetric unit. However, being only weakly bound to the rest of the structure, was found heavily disordered, with electron density surrounding the central N atom being described by a rather irregular polyhedron of six oxygen atoms of partial occupancy.

Since the silver(I) ions are chelated by four nitrogen atoms from two MBDA ligands the geometric parameter for four-coordinate compounds, τ, proposed by Alvarez and Avnir [23] was applied to AgMBDA complex and both Ag1 and Ag2 fall in distorted tetrahedron geometry, since both torsion angles between chelate planes are 70.1° and 70.7°.

Table 3
Crystallographic data for AgMBDA.

Compound	AgMBDA
Molecular formula	$Ag_2C_{72}H_{80}N_{10}O_{14}$
Formula weight (g mol^{-1})	1525.2
Crystal system	monoclinic
Space group	*C*2/*c*
a (Å)	17.9282(4)
b (Å)	17.9479(3)
c (Å)	22.5421(5)
β (°)	104.996(2)
V (Å^3)	7006.4(2)
Z	4
Crystal size (mm)	0.49 × 0.46 × 0.05
D_{calc} (g cm^{-3})	1.446
μ (Mo Kα) (cm^{-1})	0.631
Transmission factors (min/max)	0.70193/1.00000
Reflections measured/unique	33 070/8841
Observed reflections [$F^2_{obs} > 4\sigma(F^2_{obs})$]	5556
No. of parameters refined	472
$R(F_0)$	0.0361
WR (F_0^2)	0.0941
S	0.993
RMS (e$^-$ Å^{-3})	0.052

Table 4
Selected bonds and angles for AgMBDA compound.

Silver coordination sphere			
Bond (Å)			
Ag1 N1	2.297(2)	Ag2 N3	2.317(2)
Ag1 N2	2.355(2)	Ag2 N4	2.336(2)
Angle (°)			
N1 Ag1 N2	77.14(7)	N4 Ag2 N4	77.01(7)
N1 Ag1 N1	119.44(7)	N3 Ag2 N3	77.35(7)
N1 Ag1 N2	137.98(7)	N3 Ag2 N4	137.70(7)
N2 Ag1 N2	117.89(6)	N3 Ag2 N4	118.83(7)

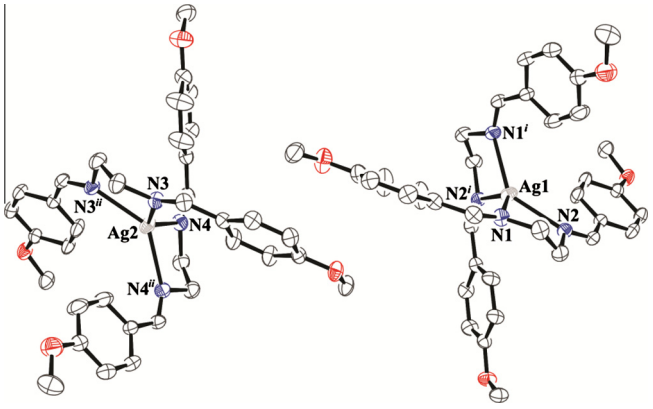

Fig. 3. ORTEP representation of crystal structure of AgMBDA. The thermal ellipsoids are drawn at 30% probability. Symmetry code: *i*(1 − *x*,*y*,1,5 − *z*) and *ii*(1 − *x*,*y*,2,5 − *z*). The hydrogen atoms and nitrate ions were omitted for the better visualization.

The Ag–N distances found fall 2.29–2.35 Å range and the distances are similar to the typical values found for other four-coordinated Ag(I) complexes containing *N*-heterocyclic ligands [24]. The main difference between these units is the angle between the aromatic rings of the ligands. For the block that contain Ag1 the angles formed between the rings of the same ligand is around 28.6° and the average is 72.4° for different ligands. For the Ag2 cationic block the angles are 38.7° and 14.24° to the same ligand and an average of 69.4° between different ligands. The cationic block charges are neutralized by two nitrate anions present in the structure. In addi-

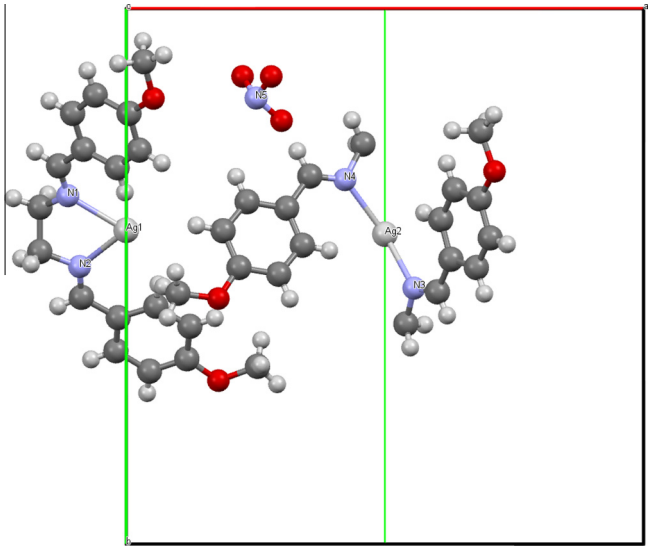

Fig. 4. The asymmetric unit of the AgMDBA crystal, showing two differently oriented half complex cations (bisected by crystallographic twofold axes, see text) and nitrate group viewed along the *c* axis. The silver and nitrate atoms are numbered. The twofold axes are in green lines. Carbon, oxygen and hydrogen atoms were colored as dark gray, red and light gray, respectively. The disordered atoms of the nitrate ion are not shown. (Color online.)

tion, non conventional hydrogen bonds C–H···O are responsible to build two different 1D networks with different orientations. The interaction of C18–H18A···O2, and C19–H19A···O3 gives rise to a one-dimensional network viewed along the *b*- and *a*-axis, respectively, see Fig. 5. Since AgMBDA is a monometallic complex, no Ag–Ag interaction was observed.

3.5. Molecular modelling

The geometry of AgMBDA was optimized by theoretical calculations using density functional theory (DFT). The calculated Ag–N bond distance was 2.420 Å, while the N1–Ag–N2 and N1–Ag–N2′ angles were 76.2° and 129.7°, respectively. Detailed bond distances, angles and dihedrals are provided as Supplementary material.

Table 5
MIC values of compounds, silver nitrate and SSD.

Compound	MIC ($\mu g\ mL^{-1}$)	% Silver	Molar mass ($g\ mol^{-1}$)	MIC ($\mu mol\ L^{-1}$)
MBDB	25		310.4	80.5
AgMBDB	11.3	22.4	480.3	23.5
MBDA	25		296.4	84.4
AgMBDA	21.2	14.1	762.6	27.8
$AgNO_3$	12.5	63.5	169.9	73.6
SSD	12.5	30.2	357.1	35.0

3.6. Antibacterial assays

The minimum inhibitory concentrations (MIC) for the two ligands and their silver(I) complexes, as well as the MIC values for $AgNO_3$, silver sulfadiazine – SSD and isoniazid, are presented in Table 5. The MBDA and MBDB molecules show low activity against *M. tuberculosis*. The silver(I) complexes were shown to be more effective than the free ligands. The MIC values found for AgMBDA and AgMBDB complexes were 27.8 and 23.5 $\mu mol\ L^{-1}$, respectively, are lower than two recently published Pt(II) complexes with *N*-, *S*-donor ligand described in literature for the same mycobacterium species [25]. The two Ag(I) complexes also possess higher activity than free $AgNO_3$. Furthermore, the AgMBDA and AgMBDB complexes have 14.1% and 22.4% of silver in their compositions, while $AgNO_3$ has 63.5%. These data suggest a synergism between Ag(I) ions and the free ligand. As described in Table 5, the two complexes are more effective than the SSD complex.

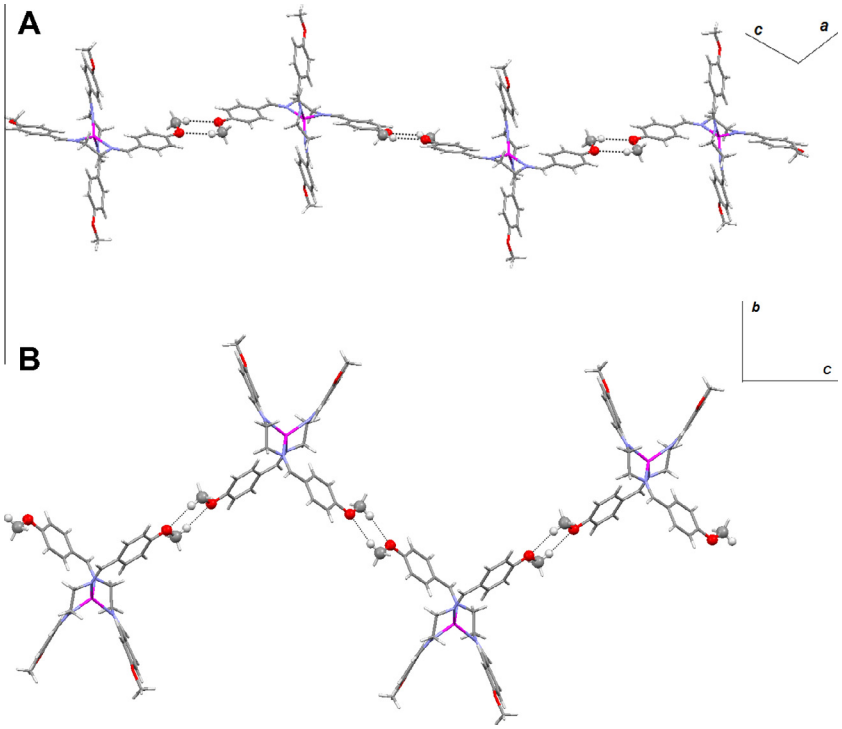

Fig. 5. 1D representation network of AgMBDA. Viewed along (a) *b*-axis and (b) *a*-axis.

4. Conclusions

Two new Schiff bases, MBDA and MBDB, and their silver(I) complexes were obtained and structurally characterized. Based on the elemental and thermal analyses, the molecular formula of AgMBDA and AgMBDB complexes were found to be $[Ag(C_{18}H_{20}N_2O_2)_2]NO_3$ and $[Ag(C_{19}H_{22}N_2O_2)NO_3]\cdot\frac{1}{2}H_2O$, respectively. Spectroscopic studies confirmed the coordination of the ligands to the silver(I) ions through the nitrogen atoms. The structure of the AgMBDA complex was determined by X-ray crystallographic analysis. Unfortunately, species AgMBDB could be isolated only as polycrystalline material, nor amenable to conventional single-crystal diffraction analysis. Studies are in progress to unravel its structure by state-of-the-art powder diffraction methods, using advanced global optimization techniques. Antimicobacterial studies have shown that both complexes are more effective than silver–sulfadiazine (SSD) and the free ligands against *M. tuberculosis*.

Acknowledgments

The authors thank FAPEMIG/Brazil processes – CEX-APQ-00173/09; 02967/10 and 00256/11 CNPq/FAPESP/Brazil – 2012/08230-2, 2009/06499-1 and 2011/11593-7, for financial support. The authors are grateful to Professor Carol H. Collins for the English revision of the manuscript.

Appendix A. Supplementary data

CCDC 897808 contains the supplementary crystallographic data for this paper. These data can be obtained free of charge via http://www.ccdc.cam.ac.uk/conts/retrieving.html, or from the Cambridge Crystallographic Data Centre, 12 Union Road, Cambridge CB2 1EZ, UK; fax: +44 1223-336-033; or e-mail: deposit@ccdc.cam.ac.uk. Supplementary data associated with this article can be found, in the online version, at http://dx.doi.org/10.1016/j.poly.2013.06.031.

References

[1] H.J. Klasen, Burns 26 (2000) 117.
[2] R. Rowan, T. Tallon, A.M. Sheahan, R. Curran, M. McCann, K. Kavanagh, M. Devereux, V. McKee, Polyhedron 25 (2006) 1771.
[3] J.M.T. Hamilton-Miller, H. Shah, Int. J. Antimicrob. Agent 7 (1996) 97.
[4] A. Melaiye, R.S. Simons, A. Milsted, F. Pingitore, C. Wesdemiotis, C.A. Tessier, W.J. Youngs, J. Med. Chem. 47 (2004) 973.
[5] WHO/HTM/TB/2009-420.
[6] A. Cuin, A.C. Massabni, C.Q.F. Leite, D.N. Sato, A. Neves, B. Szpoganicz, M.S. Silva, A.J. Bortoluzzi, J. Inorg. Biochem. 101 (2007) 291.
[7] G.S.M. Costa, P.P. Corbi, C. Abbehausen, A.L.B. Formiga, W.R. Lustri, A. Cuin, Polyhedron 34 (2012) 210.
[8] G.A. Pereira, A.C. Massabni, E.E. Castellano, L.A. Sodré-Costa, C.Q.F. Leite, F.R. Pavan, A. Cuin, Polyhedron 38 (2012) 291.
[9] A. Cuin, A.C. Massabni, G.A. Pereira, C.Q.F. Leite, F.R. Pavan, R. Sesti-Costa, T.A. Heinrich, C.M. Costa-Neto, Biomed. Pharm. 65 (2011) 334.
[10] V.Z. Mota, G.S.G. de Carvalho, P.P. Corbi, F.R.G. Bergamini, A.L.B. Formiga, R. Diniz, M.C.R. Freitas, A.D. da Silva, A. Cuin, Spectrochim. Acta, Part A 99 (2012) 110.
[11] J.L. Sessler, P.J. Melfi, G.D. Pantos, Coord. Chem. Reviews 250 (2006) 816.
[12] CRYSALISPRO, Oxford Diffraction Ltd., Version 1.171.33.41 (release 06–05-2009 CrysAlis 171.NET).
[13] G.M. Sheldrick, Acta Crystallogr., Sect. A 64 (2008) 112.
[14] A.C. Larson, Crystallogr. Comp. (1970) 291.
[15] L. Farrugia, J. Appl. Crystallogr. 45 (2012) 849.
[16] C.F. Macrae, I.J. Bruno, J.A. Chisholm, P.R. Edgington, P. McCabe, E. Pidcock, J. Appl. Crystallogr. 41 (2008) 466.
[17] L.A. Collins, S.G. Franzblau, Antimicrob. Agents Chemother. 41 (1997) 1004.
[18] J.C. Palomino, A. Martin, M. Camacho, H. Guerra, J. Swings, F. Portaels, Antimicrob. Agents Chemother. 46 (2002) 2720.
[19] M.W. Schmidt, K.K. Baldridge, J.A. Boatz, S.T. Elbert, M.S. Gordon, J.H. Jensen, J. Comput. Chem. 14 (1993) 1347.
[20] P.J. Hay, W.R. Wadt, J. Chem. Phys. 82 (1985) 299.
[21] (a) R. Ditchfie, W.J. Hehre, J.A. Pople, J. Chem. Phys. 54 (1971) 724;
(b) M.M. Francl, W.J. Pietro, W.J. Hehre, J.S. Binkley, M.S. Gordon, D.J. DeFrees, J.A. Pople, J. Chem. Phys. 77 (1982) 3654;
(c) P.C. Harihara, J.A. Pople, Theor. Chim. Acta 28 (1973) 213;
(d) W.J. Hehre, R. Ditchfie, J.A. Pople, J. Chem. Phys. 56 (1972) 2257.
[22] (a) A.D. Becke, J. Chem. Phys. 98 (1993) 5648;
(b) C.T. Lee, W.T. Yang, R.G. Parr, Phys. Rev. B 37 (1988) 785.
[23] S. Alvarez, D. Avnir, Dalton Trans. (2003) 562.
[24] C. Fan, C.B. Ma, C.N. Chen, F. Chen, Q.T. Liu, Inorg. Chem. Commun. 6 (2003) 491.
[25] P.I.S. Maia, A. Graminha, F.R. Pavan, C.Q.F. Leite, A.A. Batista, D.F. Back, E.S. Lang, J. Ellena, S.S. Lemos, H.S.S. Araujo, V.M. Deflon, J. Braz. Chem. Soc. 21 (2010) 1177.